MANSOURA JOURNAL OF Physics
Official Journal of Faculty of Science, Mansoura University, Egypt
E-mail: scimag@mans.edu.eg ISSN: 2974-4954

The role of selenium oxide substitution in lead phosphate glasses

F. Amghar[a, b*], A.M. Abdelghany[c], R.M Shalaby[a]

[a]*Physics Department, Faculty of Science, Mansoura University, Mansoura, 35516, Egypt.*

[b]*Physics Department, Faculty of Ghat,, Sabha University, Sabha, Libya*

[c]*Spectroscopy Department, Physics Division, National Research Center, 33 Elbehouth St., Dokki, 12311, Giza, Egypt.*

Received:16/12/2021
Accepted:19/12/2021

Abstract: A new lead phosphate glasses containing different concentrations of SeO_2 in the system 40PbO-(60-*x*) P_2O_5-*x*SeO_2 (*x* = 0, 2, 4, 6, 7, 8, 9, 10, and 15 mol%) were synthesized via traditional melt quenching technique. X-ray diffraction spectra of all prepared glass samples have revealed the formation of an ordinary amorphous phase. The replacement of P_2O_5 by SeO_2 causes a change of the oxygen bonding in the glasses network leading to enhancements of the polymerization process. The formation of pyrophosphate (Q_1) species with increasing SeO_2 content are the main reason for such a polymerization process. The structural groups in the resultant glass structure were determined using Fourier transform infrared (FT-IR) spectroscopy. The density, molar volume, packing density as well as free volume were determined and discussed. The dual role of selenium ions is prominently reflected on the local structure, which is dominated in this case by pyrophosphate units, for SeO_2 content greater than 5 mol%..

keywords: Lead Phosphate glass; selenium oxide, Density; FTIR Spectroscopy.

1. Introduction

Phosphate-based oxide glasses are a type of vitreous system with distinct physical and chemical characteristics [1,2]. These characteristics including high transparency [3], low melting point [4], high thermal expansion coefficients [5], low refractive index, and dispersion [6], mark these glasses as a potential candidate for several and extended applications. These applications included nuclear waste [6], medical field [7], solid electrolyte [8], sealing candidates [9], security optics, sensing and laser technologies [10], and dielectric field [11] based upon glass compositions and diversity of their properties. The structure of P_2O_5 differs from the other important glass formers, B_2O_3 and SiO_2 [12]. Phosphate glasses are inorganic vitreous materials, where the network of phosphate glass is of polymeric nature, built by the linkage between PO_4 tetrahedra that form the backbone of the structure and is influenced by the glass composition [13]. The addition of modifier oxide to the glass composition creates a modifier region in the network structure depending on the concentration and the type of the modifiers [13]. In the modified network, the non-bridging oxygen link covalent to ionic regions. This region can provide a useful picture which describes the occurs change in composition due to ionic conductivity [12, 13]. Glasses have been modified with several trace elements in recent years, including Co, Zn, Cr, Cu, Ca, and Sr [14]. The crystal structure, solubility, thermal stability, specific surface, morphology, biological and physicochemical characteristics of glasses can all be affected by these ions [14]. Lead phosphate glass has technological importance due to its unique properties including excellent radiation shielding, low melting temperature, .etc. [15, 16]. The structure of lead borate glasses was extensively studied [15-17]. The existence of PbO may lead to an enhancement of the chemical durability resulting from the formation of P-O-Pb bonds [17]. Depending on the concentration of PbO, the structural role of PbO has an intermediate character between modifier (<15 mol% PbO), the mixed role of network modifier and network former (40-70 mol% PbO), and acts as former (70-80 mol %) [17]. The existence of PbO causes a variation in the short-range ordering structure of the phosphate glass network and converting

phosphate groups from meta-phosphate to pyrophosphate groups with increasing PbO content [18]. Selenite glasses can also be used for a variety of purposes like supersonic semiconductors, nonlinear optical devices, sensors, solar cells, and photocells reflecting windows [19-20]. Besides, adding of SeO_2 causes a change on the optical properties and decreases of melting point of the glass [21]. Introduce SeO_2 into phosphate glasses causes the depolarization process of the glass network, it is more evidence on the sample surface than deeper layers of the samples [22]. Due to the addition of SeO_2 in Ag_2O-SeO_2-B_2O_3 glasses, the S-O- bonds and isolated SeO_3 units forms during the formation glass network, and create non bridging oxygen bonds [23]. This study aims to investigate the role of SeO_2 on the structural, physical and optical properties of lead phosphate glass.

2. Experimental Work

2.1. Sample preparation

Binary lead phosphate glass samples containing different amounts of selenium oxide were synthesized using the traditional melt quenching route. The series of the 40PbO-(60-*x*) P_2O_5-*x*SeO_2 (*x* = 0, 2, 4, 6, 7, 8, 9, 10, and 15 mol%) phosphate glasses were successfully synthesized by mixing the basic raw chemicals which include SeO_2, PbO, and $NH_4H_2PO_4$ as a source of P_2O_5, see Table 1. The used chemicals were all of the analytical grades with a purity of 99.9 % (Aldrich Company). All components were weighted using a micro-analytical balance and mixed according to molar composition proportions; then they melted in a 50 ml porcelain crucible at 300 ^{0}C for 30 min to remove NH_3 and H_2O. The applied melting temperature is 1000 ^{0}C for approximately 1 h depending on the composition of the glasses. The mixed of all components together causes decreases in the melting temperature and avoids volatility of SeO_2. To get homogeneous synthetic samples, the melt is swirled many times. To acquire the appropriate samples, the melted samples were put into a heated stainless steel mold.

Glass samples were formed using analytical grade chemicals of Silicon dioxide SiO2 supplied by LANXESS, Germany. Boron oxide used in the form of boric acid H_3BO_3 supplied by El-Gomhouria Co. P_2O_5 was introduced in the form of Ammonium dihydrogen orthophosphate supplied by LANXESS Co. CaO and Na_2O were introduced in their carbonate form and supplied by EL-Nasr pharmaceutical chemicals Co. All previously mentioned chemicals were used to synthesize glassy samples with a composition shown in Table (1). The batches were melted in porcelain crucibles within a programmable electrical furnace regulated at 1100–1200 ^{o}C. Molten glass was occasionally stirred many times to ensure the formation of homogenized bubble-free glasses. To eliminate thermal and internal stresses, the molten glass was cast onto warmed stainless steel plates of the appropriate size, annealed for 1 hour, and then cooled gently to room temperature.

Table 1: Sample appointment and composition

Sample	PbO	P_2O_5	SeO_2
	mol%		
G_0	40	60	0
G_2	40	58	2
G_4	40	56	4
G_6	40	54	6
G_7	40	53	7
G_8	40	52	8
G_9	40	51	9
G_{10}	40	50	10
G_{15}	40	45	15

2.2.Characterization and parameter calculations

X-ray spectroscopy technique is utilized to determine whether the material is amorphous or crystalline in nature. Diffraction patterns of XRD were recorded via Brucker Axs-D8 Advance, employing CuKα radiation of wavelength 0.15406 nm within Bragg angles extended between 3-70° with a step 0.02°.

The FTIR spectral data were obtained using KBr pellets method within the spectral range-extended between 4000-400 cm^{-1} via Nicolet is10 FTIR single beam spectrometer adopting 2 cm^{-1} spectral resolution. The spectrum of every sample is collected through a collection of 32 scans. The acquired spectrum was normalized and corrected for background and dark current noises.

The density (*D*) of the investigated samples was measured at ordinary room temperature adopting Archimedes principle using xylene as an immersion liquid using 4-digits electronic

balance using the formula previously published [24]:

$$D = \frac{W_{SA}}{W_{SA}-W_{SL}} \times D_L \qquad (1)$$

where D is the density of the sample, W_{SA}, W_{SL}, and D_L are weights of sample in the air, sample in liquid, and density of immersion fluid respectively. The measurements were performed and averaged for triplicate samples from each composition with a random error of about ±0.02 g/cm^3.

The volume occupied by a mol glass named molar volume (V_m) can be calculated as [25]:

$$V_m = \sum \frac{M_i n_i}{D} \qquad (2)$$

where M_i is the molecular weight for the component i. n_i is the molar ratio. D is the glass density.

Packing density (P_d) and free volume (V_f) were evaluated using the following equation respectively [25]:

$$V_f = V_m - \sum x_i V_i \qquad (3)$$

$$P_d = \sum \frac{x_i V_i}{V_m} \qquad (4)$$

3. Results and Discussion

3.1. X-ray analysis

Fig. 1 shows the X-ray diffraction spectra of all prepared glass samples.

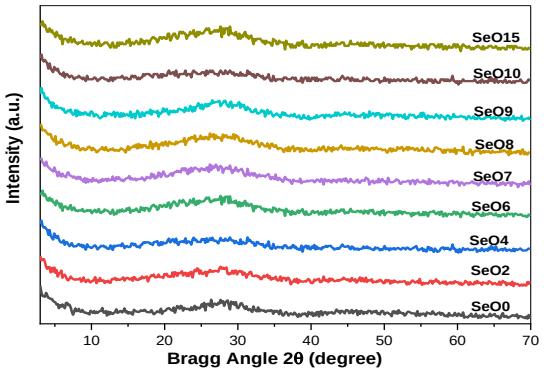

Fig.1. X-ray spectra of all prepared glass samples

These patterns show the absence of any sharp diffraction peaks with a halo centered at about 28° that confirmed the amorphous nature of the studied glasses containing different content of selenium oxide.

3.1. FTIR optical absorption spectra

Fig. 2 displays the FTIR experimental data of the lead phosphate base glass beside other samples that containing CeO_2 contents. The addition of selenium oxide (x = 2, 4, 6, 7, 8, 9, 10, and 15 mol%) to the glass matrix composition causes minor changes in the FTIR spectra. FTIR data is correlated with previous studies [29] and confirm significant depolymerization in the phosphate network with the addition of 40 mol% of PbO as well as different contents of SeO_2.

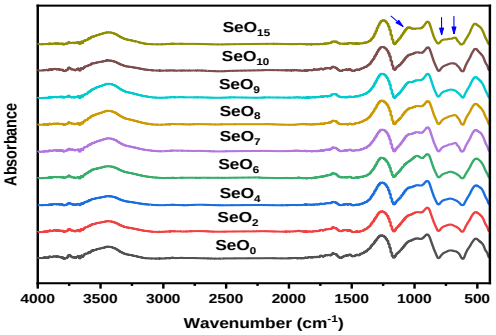

Fig.2. displays FTIR spectra of all prepared glass samples.

Table 2: Peaks position and bands assignment of FTIR and Raman spectra for investigated samples

Center(cm^{-1})	Assignment	Ref.
500-525	Bending vibrations of O-P-O units overlapped with S-O-vibration	[30]
650-800	Symmetric and asymmetric stretching vibrations respectively of P-O-P bonding	[31]
800-1050	NBO of PO_4 & vibration of SeO_3 units	[33]
1250	Vibration mode of the O-P-O bonding, denoted by $\nu_{as}(PO_2)$-	[33]
1650 & 3440	OH, PO vibrations	[32]

The lengthy chain is shortened as a result, and the phosphate glass structure is made up of a shorter Q_2 chain and Q_1 tetrahedral structural unit. The infrared spectrum shows distinct vibrational bands, most of which appear to be in the fingerprint region as characteristic of vibrational units. A strong far IR broadband is observed at 512 cm^{-1} is assigned to the bending vibrations of O-P-O units overlapped with S-O-vibration [30].

A medium band is identified at about 714 cm^{-1}, and a strong band with two peaks appearing around 900 and 980 cm^{-1} are attributed to the symmetric and asymmetric stretching vibrations respectively of P-O-P bonding [31]. Also, a strong band is shown about 1265 cm^{-1} is assigned to asymmetric stretching vibration mode of the O-P-O bonding, denoted by $\nu_{as}(PO_2)$-. A small band is

identified at about 1650 cm^{-1}, and a band is observed at about 3447 cm^{-1} are due to the water, OH, POH vibrations [32]. At high content of SeO_2 (x= 15 mol%), broadband at about 714 tends to separate which indicates that SeO_3 units formed as well as appeared in the small band at about 1050 cm^{-1} [30]. The position and assignment of these bands are recorded in Table 2.

3.3. Calculated physical parameters

The density of all prepared samples was measured at room temperature using Archimedes' method. Three samples were taken from each glass and the measurements values were listed in Table 3. Fig. 3 shows a mostly no change in both density and molar volume with incorporation SeO_2 contents, despite the formation of SeO_3 and PbO_4 units. In which PbO_4 units have the greatest density among the structural units [29].

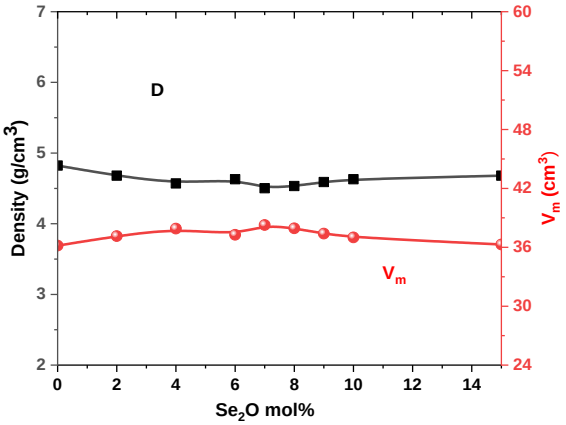

Fig.3. Density and molar volume of studied glass

These trends can be explained simply by the practically constant molecular mass of glasses. The correlation between these quantities, on the other hand, is inextricably linked to the structural units of glass, namely their concentration, mass, and volume [35]. It is also concluded that the changes in the volume of the formation structural units nearly compensate for each other.

Free volume and packing density were evaluated and recorded in Table 3. It is observed from fig. 4 that packing density decreases with the replacement of P_2O_5 with SeO_2 due to its modifier role that causes a depolarization process of the glass network. Conversely, the free volume is increased

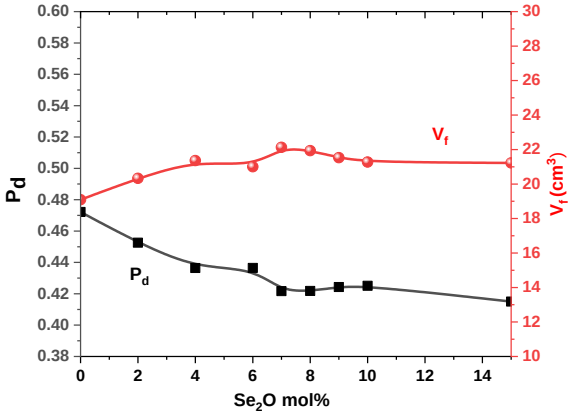

Fig.4. The packing density and free volume of all prepared glass samples as a function of SeO_2 concentrations

4. Conclusions

Lead phosphate glass containing different contents of SeO_2 was successfully prepared via the traditional melt quenching method and has been studied using different structural techniques. XRD spectra revealed the polycrystalline nature of all prepared samples. The addition of SeO_2 contents affects the crystalline process. The crystalline degree increases with increasing SeO_2 concentration and the crystalline phase is formed. The glass density slightly changes due to the dual role of SeO_2 and the replacement of the low density of P_2O_3 (2.2g/mol) by higher density SeO_2 (3.2 g/mol). The decrease of oxygen atoms number in the glass network with the addition SeO_2 leads to decreases in the packing density. The Vickers hardness values are increased which are in good agreement with the XRD result.

Table 3: Physical parameters of all prepared glass samples

Physical Parameters	Glass code								
	G_0	G_2	G_4	G_6	G_7	G_8	G_9	G_{10}	G_{15}
Density	4.73	4.80	5.03	4.84	5.01	5.05	4.92	5.06	4.73
Molar Volume	36.55	35.82	33.91	35.09	33.75	33.40	34.16	34.16	36.55
Packing Density	0.47	0.45	0.44	0.44	0.42	0.42	0.42	0.42	0.41
Free Volume	19.09	20.33	21.36	21.00	22.13	21.93	21.53	21.27	21.22

5. References

1 Metwalli E., M. Karabulut, D. L. Sidebottom, M. M. Morsi, and R. K. Brow, (2004) "Properties and structure of copper ultraphosphate glasses," *J. Non. Cryst. Solids*, **344**, no. 3, pp. 128–134,.

2 Abdelghany A. M., G. El-Damrawi, A. H. Oraby, and M. A. Madshal, (2018). "Optical and FTIR structural studies on CoO-doped strontium phosphate glasses," *J. Non. Cryst. Solids*, **499**, pp. 153–158,

3 Makhlouk R., N. Beloued, and S. Aqdim, (2018.) "Study of Chromium-Lead-Phosphate Glasses by XRD, IR, Density and Chemical Durability," *AdvMater. Phys. Chem*. **8**, no. 6, pp. 269–280,

4 Beloued N., Z. Chabbou, and S. Aqdim, (2016). "Correlation between Chemical Durability Behaviour and Structural Approach of the Vitreous Part of the System $55P_2O_5$-$2Cr_2O_3$-(43-x) Na_2O-xPbO," Adv. Mater. Phys. Chem., **6**(6), pp. 149–156,

5 Abd El-Ati M. I. and A. A. Higazy, (2000) "Electrical conductivity and optical properties of gamma-irradiated niobium phosphate glasses," *J. Mater. Sci.*, **35**, no. 24, pp. 6175–6180

6 Bergo P., S. T. Reis, W. M. Pontuschka, J. M. Prison, and C. C. Motta, (2004) "Dielectric properties and structural features of barium-iron phosphate glasses," *J. Non. Cryst. Solids*, **336**, no. 3, pp. 159–164

7 Abdelghany A. M. and H. Kamal, (2014). "Spectroscopic investigation of synergetic bioactivity behavior of some ternary borate glasses containing fluoride anions," Ceram. Int., **40**, no. 6, pp. 8003–8011,

8 Makhkhas, Y., Aqdim, S., & Sayouty, E. H. Study of sodium-chromium-iron-phosphate glass by XRD, IR, Chemical Durability and SEM. *Technical Proceedings of the 2013 NSTI Nanotechnology Conference and Expo, NSTI-Nanotech* 2013.

9 Wei, T.Y., Hu, Y. and Hwa, L.G. (2001) Structure and Elastic Properties of Low-Temperature Sealing Phosphate Glasses. *Journal of Non-Crystalline Solids*, **288**, 140-147.

10 El-Damrawi G., A. M. Abdelghany, A. H. Oraby, and M. A. Madshal, (2020) "Structural and optical absorption studies on Cr_2O_3 doped SrO-P_2O_5 glasses," Spectrochim. *Acta Part A Mol. Biomol. Spectrosc.*, **228**, p. 117840,.

11 Kumar S., P. Vinatier, A. Levasseur, and K. J. Rao, (2004). "Investigations of structure and transport in lithium and silver borophosphate glasses," *J. Solid State Chem.*, **177**, no. 4–5, pp. 1723–1737,

12 El-Damrawi G., A. M. Abdelghany, and M. A. Madshal, (2021) "AC conductivity and dielectric properties of Cr_2O_3 doped SrO–P2O5 glasses," *Phys. B Condens. Matter*, **618**, p. 413184,.

13 Abdelghany A. M., G. El-Damrawi, A. H. Oraby, and M. A. Madshal, (2019.)"AC conductivity and dielectric properties of CoO doped SrO-P_2O_5 glasses," *Phys. B Condens. Matter*, **573**, pp. 22–27,

14 Forrer R., K. Gautschi, and H. Lutz, (2001). "Simultaneous measurement of the trace elements Al, As, B, Be, Cd, Co, Cu, Fe, Li, Mn, Mo, Ni, Rb, Se, Sr, and Zn in human serum and their reference ranges by ICP-MS," Biol. *Trace Elem. Res.*, **80**(1), pp. 77–93,

15 Kilic G., E. Ilik, K. A. Mahmoud, R. El-Mallawany, F. I. El-Agawany, and Y. S. Rammah, (2020). "Novel zinc vanadyl boro-phosphate glasses: ZnO–V_2O_5–P_2O_5–B_2O_3: physical, thermal, and nuclear radiation shielding properties," *Ceram. Int.*, **46**, no. 11, pp. 19318–19327,

16 Arbuzov V. I., N. Z. Andreeva, N. A. Leko, S. I. Nikitina, N. F. Orlov, and Y. K. Fedorov, (2005) "Optical, spectral, and radiation-shielding properties of high-lead phosphate glasses," *Glas. Phys. Chem.*, **31**, no. 5, pp. 583–590,.

17 Kavaz E., H. O. Tekin, N. Y. Yorgun, Ö. F. Özdemir, and M. I. Sayyed, (2019). "Structural and nuclear radiation shielding properties of bauxite ore doped lithium borate glasses: experimental and Monte Carlo study," *Radiat. Phys. Chem.*, **162**, pp. 187–193,

18 Laorodphan N., (2012) "Structural studies of thallium containing germanate and borate glasses and crystalline phases."

University of Warwick,.
19 Bachvarova-Nedelcheva A., R. Iordanova, and Y. Dimitriev, (2009) "Optical properties of selenite glasses," *J. Non. Cryst. Solids*, **355**, no. 37–42, pp. 2027–2030,.
20 Abe M., Y. Benino, T. Fujiwara, T. Komatsu, and R. Sato,(2005.) "Writing of nonlinear optical Sm 2 (Mo O 4) 3 crystal lines at the surface of glass by samarium atom heat processing," *J. Appl. Phys.*, **97**, no. 12, p. 123516,.
21Dimitriev Y., St. Yordanov b, L. Lakov (200 1). "The structure of oxide glasses containing SeO2," *J. Non. Cryst. Solids*, **293**, pp. 410–415,
22 Ciceo-Lucacel R., M. Todea, and V. Simon, 2018 "Effect of selenium addition on network connectivity in P_2O_5-CaO-MgO-Na_2O glasses," *J. Non. Cryst. Solids*, **488**, pp. 10–13,.
23 Palui A. and A. Ghosh, (2018) "Structure and dielectric properties of Ag_2O-SeO_2-TeO_2 mixed former glasses," *J. Non. Cryst. Solids*, **482**, pp. 230–235.
24 El-Damrawi G., A. M. Abdelghany, M.Abdelghany, and M. A. Madshal (2021). "Structural role of chromium sulfate in modified borate glasses and glass ceramics," *Materialia*, **16**, p. 101095,
25 Madshal M. A., G. El-Damrawi, A. M. Abdelghany, and M. I. Abdelghany, (2021). "Structural studies and physical properties of Gd_2O_3-doped borate glass," *J. Mater. Sci. Mater. Electron.*, **32**, pp. 1–12.
26 Chandler H., (1999) "Introduction to hardness testing," Hardness testing. *USA ASM Int.*, pp. 1–13.
27 Marzouk M. A., H. A. ElBatal, and R. L. Elwan, (2019) "Effect of MoO_3, MnO_2 or mixed dopants on the spectral properties and crystallization behavior of sodium phosphate glasses containing either MgO or MgF_2," *Appl. Phys. A*, **125**(6), pp. 1–11.
28 Brow R. K., (2000.), "The structure of simple phosphate glasses," *J. Non. Cryst. Solids*, **263**, pp. 1–28.
29 El-Egili K., H. Doweidar, Y. M. Moustafa, and I. Abbas, (2003) "Structure and some physical properties of PbO–P_2O_5 glasses," *Phys. B Condens. Matter*, **339** (4), pp. 237–245.
30 Marzouk M. A., A. M. Fayad, and H. A. ElBatal, (2017). "Correlation between luminescence and crystallization characteristics of Dy^{3+} doped P_2O_5–BaO–SeO_2 glasses for white LED applications," *J. Mater. Sci. Mater. Electron.*, **28**, no. 17, pp. 13101–13111.
31 Dimitriev Y. B., S. I. Yordanov, and L. I. Lakov, (1995). "Formation and structure of glasses containing SeO_2," *J. Non. Cryst. Solids*, **192**, pp. 179–182.
32 Ibrahim S. and M. A. Marzouk, (2017). "Structural characteristics and electrical conductivity of vanadium-doped lithium ultraphosphate glasses," *Silicon*, **9**(3), pp. 403–410.
33 Deb B., Ionic Glasses and Nanocomposites: Theory and Experiments. *Educreation Publishing*, 2018.
34 Samanta B., D. Dutta, and S. Ghosh, (2017). "Synthesis and different optical properties of Gd_2O_3 doped sodium zinc tellurite glasses," *Phys. B Condens. Matter*, **515**, pp. 82–88.
35 Brauer D. S., A. Al-Noaman, R. G. Hill, and H. Doweidar, (2011) "Density–structure correlations in fluoride-containing bioactive glasses," *Mater. Chem. Phys.*, **130**(1–2), pp. 121–125.
36 Ahmed E. M., N. A. El-Ghamaz, and S. M. Albhbah, (2020) "Effect of Nd^{3+} ions on the structural, physical and emission properties of some As_2O_3. V_2O_5. CuO glasses," *Ceram. Int.*, **46**(16), pp. 25089–25096.